A NEW METHOD FOR ASSESSING THE SAFETY OF SHIPS DAMAGED BY GROUNDING

(DOI No: 10.3940/rina.ijme.2012.a1.218)

J.K. Paik, **D.K. Kim**, **D.H. Park**, **H.B. Kim**, Pusan National University, and **M.S. Kim**, Lloyd's Register Asia

The primary aim of the present study is to propose an innovative method for assessing the safety of ships which have suffered accidental or in-service damages. Only a small number of probable scenarios for accidental or in-service damage representing all possible damage scenarios are selected using a sampling technique in which the random variables affecting the damage are probabilistically characterized. A damage index for the corresponding damage scenario is defined as a function of damage characteristics such as location and extent of the damage. The residual strength performance of a ship with the corresponding damage scenario can then be calculated by analytical or numerical methods. Once this process has been carried out for each of the damage scenarios selected, a diagram relating the residual strength performance to the damage index (abbreviated as the R-D diagram) can be established. This diagram will be very useful for a first-cut assessment of a ship's safety immediately after it has suffered structural damage. The diagram can also be used to determine acceptance criteria for a ship's safety against accidental or in-service damage. An applied example is shown to demonstrate the applicability of the proposed method in terms of developing a diagram between the ultimate longitudinal strength versus grounding damage index for four types of double-hull oil tankers – VLCC, Suezmax, Aframax, and Panamax.

NOMENCLATURE

GDI	=	Grounding damage index, given by equation (3)
R-D diagram	=	Residual strength versus damage index diagram
B	=	Ship breadth
b	=	Double side width
D	=	Ship depth
h	=	Double bottom height
L	=	Ship length

1. INTRODUCTION

Ship collisions and grounding continue to occur regardless of continued efforts to prevent such accidents. With the increasing demand for safety at sea and for the protection of the environment, it is of crucial importance to be able to reduce the probability of accidents, assess their consequences, and ultimately minimize or prevent potential damage to ships and to the marine environment (Paik et al., 2003).

Generally, ship collisions and grounding result in structural damage, marine pollution (depending on the cargo type), and hull collapse (Paik et al., 1998). This study is concerned with hull collapse in double-hull oil tankers after grounding accidents. To facilitate the rapid planning of salvage and rescue operations of ships after grounding, the residual ultimate longitudinal strength of damaged ships must be assessed quickly and accurately, together with the location and extent of the damage.

This study proposes an innovative method for the safety assessment of ships that have suffered structural damage due to accidents. Only a small number of probable scenarios for accidental or in-service damage representing all possible damage scenarios are selected using a sampling technique in which the random variables that affect the damage are probabilistically characterized. A damage index for any given damage scenario is defined as a function of the location and extent of the damage. The residual strength performance of a ship in any given damage scenario can be identified by analytical or numerical methods.

Once this process has been carried out for each of the damage scenarios selected, a diagram relating the residual strength performance to the damage index can be established. This diagram is useful as a first-cut assessment of a ship's safety immediately after suffering structural damage. The diagram should also prove useful in determining the acceptance criteria for ship safety following accidental or in-service damage.

The proposed ultimate longitudinal strength-based safety assessment is validated by its application to double-hull oil tankers that have suffered grounding accidents. Four types of double-hull oil tankers – VLCC, Suezmax, Aframax, and Panamax – are considered.

Four random variables – grounding location in the direction of the ship's beam, grounding penetration in the vertical direction, breadth of the top of the rock (and whether it has a sharp or blunt shape), and the angle of the rock are assigned to define the extent and location of the grounding damage. The probability density function of each of the four random variables is characterized by the International Maritime Organization's (IMO's) historical database on ship grounding accidents. Fifty probable scenarios that represent all possible grounding scenarios are selected by using a Latin hypercube sampling technique with the four random variables.

The grounding damage index is defined as the sum of the damaged cross sectional area of the hull in relation to the original cross sectional area of the hull in both the outer

bottom and inner bottom structures. The contributions of the outer bottom and inner bottom to a ship's ultimate longitudinal strength differ, and thus a correction coefficient is introduced to adjust the contribution of the inner bottom structures.

The grounding damage indices can be calculated for all of the selected grounding damage scenarios. The ultimate longitudinal strength of ships suffering any given type of grounding damage is then calculated by using the modified Paik-Mansour formula method (Paik et al., 2011), which is based on the probable distribution of hull-girder bending stresses at the ultimate limit state. This method has been proven by comparison with nonlinear finite element method and test data.

Based on these computations, four diagrams relating the residual ultimate longitudinal strength of a damaged ship (normalized by the ultimate longitudinal strength of the intact ship) to the grounding damage index are established for VLCC, Suezmax, Aframax, and Panamax class tankers. Closed-form equations of the four diagrams are then formulated by curve-fitting. The difference between the four diagrams is discussed, and a formula that represents all four diagrams is developed.

The diagrams should prove useful for judging the safety level of a damaged ship in the early stages of planning for salvage and rescue operations. They will also be very useful in the development of acceptance criteria for grounding strength performance associated with certain amounts of grounding damage.

2. GENERAL PROCEDURE FOR THE DEVELOPMENT OF THE RESIDUAL STRENGTH – DAMAGE INDEX DIAGRAM

Figure 1 shows the general procedure for the development of a diagram showing the relationship between the residual strength versus the damage index (abbreviated as an R-D diagram).

Once a ship's structural topology has been defined, including geometry, dimensions, and material properties, several probable damage scenarios are selected. Probabilistic aspects of the damage parameters are identified in advance. A sampling technique can be applied to select scenarios for which the probabilistic aspects of the damage parameters are known. Considering the uncertainties of parameters involved, there must be a huge number of possible scenarios, and thus it is desirable to consider damage scenarios as many as possible to develop the R-D diagram which can represent a smaller interval of the random variables in a wider range of damage extent, but the computational cost required may limit the number to about 50 scenarios, for example.

A damage index is defined, representing the damage severity for each of the selected scenarios. The residual strength of a ship in the various damage scenarios is then calculated by a simplified method or more refined nonlinear finite element method. The diagram of residual strength versus the corresponding damage index can then be plotted based on these computations.

An applied example of the procedure is illustrated in terms of establishing a residual ultimate longitudinal strength versus grounding damage index diagram for double-hull oil tankers. It is evident that a similar diagram can of course be developed for any specific damage type and its corresponding residual strength performance and damage index.

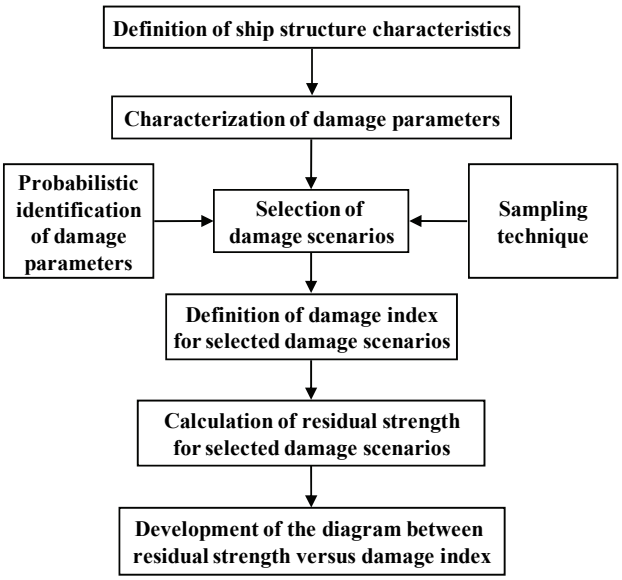

Figure 1 Flow of the proposed method for the development of the residual strength versus damage index diagram (R-D diagram)

3. PROCEDURE FOR THE DEVELOPMENT OF THE RESIDUAL ULTIMATE LONGITUDINAL STRENGTH – GROUNDING DAMAGE INDEX DIAGRAM

3.1 GROUNDING DAMAGE PARAMETERS

When a ship strikes aground on a rock, as shown in Figure 2, the resulting grounding damage can be characterized by the following four aspects.

- Location and extent (length) of damage in the direction of the ship's length.
- Location and extent (width) of damage in the direction of the ship's beam.
- Location and extent (vertical penetration) of damage in the direction of the ship's depth.
- Shape (breadth, angle) of the rock.

Historically, a large number of studies on grounding (and collision) accidents have been carried out in the literature in terms of damage predictions (Simonsen & Hansen, 2000), structural consequences (Zhang, 2002; Zhang &

Suzuki, 2006; Paik, 2007a, 2007b), hull girder collapse (Pedersen, 1994; Paik et al., 1998; Wang et al., 2000), and structural designs (Ohtsubo et al., 1994; Paik, 2003). Some recent studies on grounding accidents by Samuelides et al. (2009), Pedersen (2010), and Nguyen et al. (2011a, 2011b, 2011c), among others, may also be referred to.

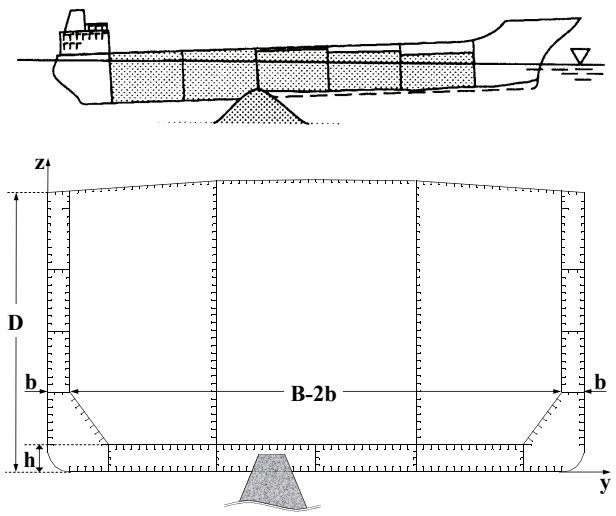

Figure 2 Ship aground on a rock

In terms of the characterization of the grounding damage associated with the residual ultimate longitudinal strength, the location and extent of grounding damage in the direction of the ship's length is not taken into account, because the analysis of the ultimate hull strength is based on the reduction of the hull cross section at the damage location and independent of the extent of the longitudinal damage.

The location and extent of damage in the directions of the ship's breadth and depth are the primary parameters that affect the longitudinal strength of the ship, and the shape of the rock in terms of breadth and tip type (e.g., blunt or sharp) governs the type of grounding damage sustained.

With this in mind, the grounding damage parameters for the residual ultimate longitudinal strength calculations can be defined as follows.

- x_1 - grounding location in the direction of the ship's beam (y).
- x_2 - height H of rock penetrating into the bottom of the hull in the direction of the ship's depth (z).
- x_3 - breadth d_1 of the bottom of the rock at the elevation corresponding to the ship's baseline and breadth d_2 of the tip of the rock.
- x_4 - angle of the rock θ,

where a triangle shaped rock is considered.

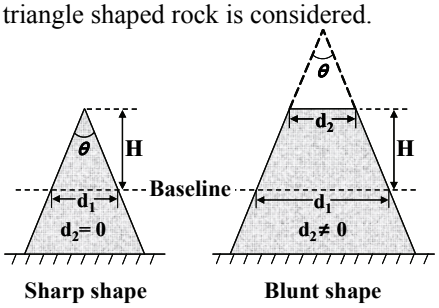

$$d_2 = d_1 - 2H \tan\frac{\theta}{2}$$

Figure 3 Nomenclature for a triangle shaped rock

3.2 DAMAGE SCENARIO SELECTION

Only a small number of the damage scenarios representing all possible damage scenarios are selected by using a sampling technique based on the probabilistic density distributions of the damage parameters.

Figures A.1 and A.2 represent the probability density distributions of the extent of grounding damage in the directions of the ship's beam and depth, respectively (Paik et al., 2003). Although the extent of the grounding damage (length) in the direction of the ship's length cannot be dealt with as a damage parameter in terms of establishing the R-D diagram, its probability density distribution is presented as shown in Figure A.2 (Paik et al., 2003). Figures A.1 to A.3 show that the probability density distributions for the parameters related to the extent of grounding damage is likely to follow a Weibull function.

The IMO (2003) specifies the probability density distributions for the grounding damage parameters x_1, x_2, and x_3 as shown in Figures 4, 5, and 6, respectively.

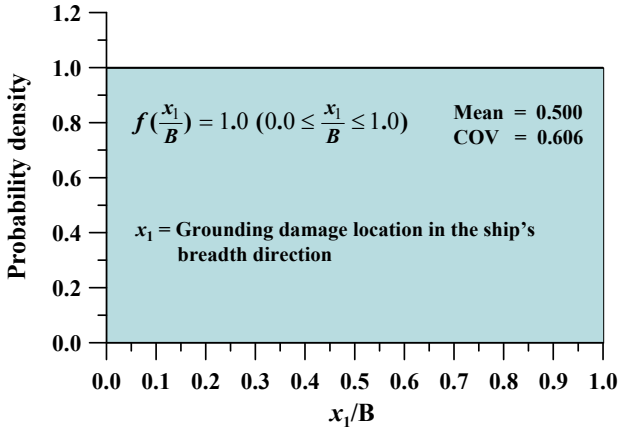

Figure 4 Probability density distribution for grounding damage location (transverse location) in the direction of the ship's breadth, normalized by ship breadth (IMO, 2003)

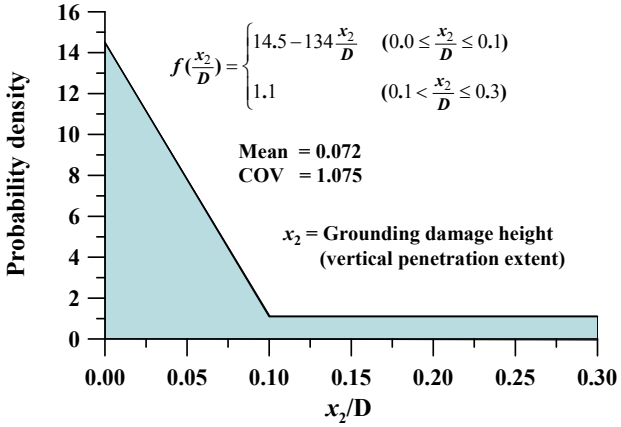

Figure 5 Probability density distribution for grounding damage height (vertical penetration extent) normalized by ship depth (IMO, 2003)

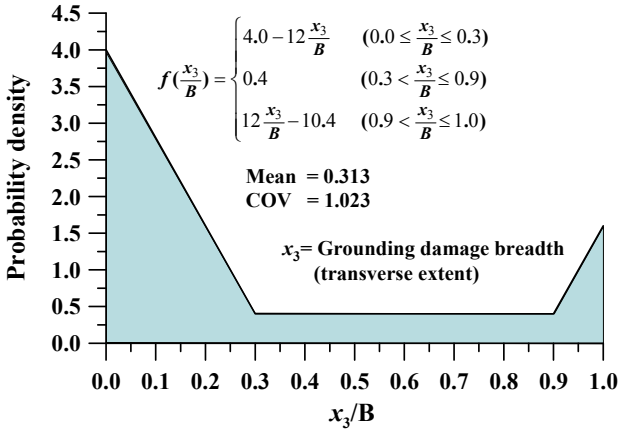

Figure 6 Probability density distribution for grounding damage breadth (transverse extent) normalized by ship breadth (IMO, 2003)

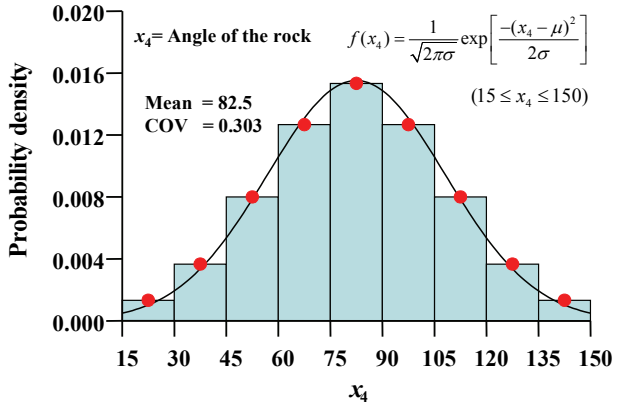

Figure 7 Probability density distribution of the assumed rock's angle

In the present study, the corresponding probability density distribution for the angle of the rock (x_4) is assumed to follow a normal function, which is plotted in Figure 7 and expressed as follows.

$$f(x_4) = \frac{1}{\sqrt{2\pi\sigma^2}} \exp\left[\frac{-(x_4-\mu)^2}{2\sigma^2}\right] \quad (15 \le x_4 \le 150) \qquad (1)$$

where μ is the mean (= 82.50), σ is the standard deviation (= 25.71), and COV is the coefficient of variation (=0.303).

The probability P of each of M samples generated by the Latin hypercube sampling technique for N variables is obtained as follows.

$$P = \left(\frac{1}{M}\right)^N \qquad (2)$$

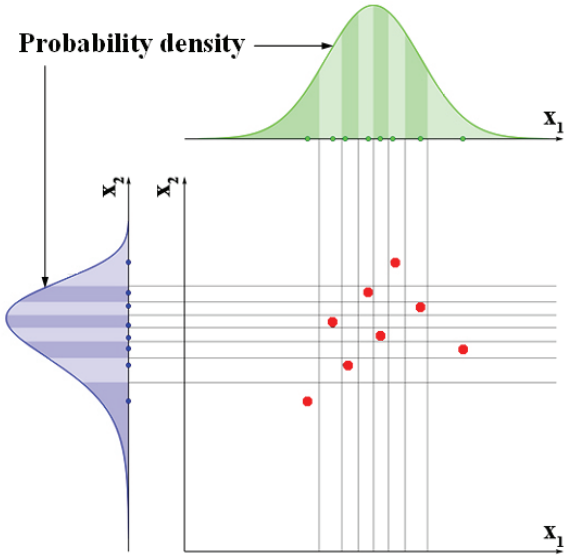

Figure 8 Illustration of the Latin hypercube sampling technique for a case with two variables and eight samples

Although a huge number of possible damage scenarios may be pertinent, it is not practical to consider all of them. A sampling technique should thus be applied to select a more limited number of probable scenarios. The Latin Hypercube Sampling (LHS) technique (Ye, 1998) is useful for efficiently selecting probable scenarios.

When sampling a function of N variables (damage parameters) using the Latin hypercube sampling technique, the range of each variable is divided into M equally probable strata (intervals), as shown in Figure 8. One sample is chosen from each stratum (e.g., assuming uniform probability over the stratum).

The M-th column in the N-th dimension of the hypercube corresponds to the value from the M-th stratum of the N-th random variable. Sample points are then placed to satisfy the Latin hypercube requirements, as shown in Figure 8. This forces the number of divisions M to be the

same for each variable. Also note that this sampling scheme does not require more samples for more dimensions (variables), which is one of its main advantages.

3.3 CALCULATION OF THE GROUNDING DAMAGE INDEX

The grounding damage index (GDI) represents the severity of grounding damage. For ships with a double bottom structure, both the inner bottom panels and the outer bottom panels can be damaged. Thus, the GDI must be defined in terms of the extent and location of grounding damage to both the outer and inner bottom structures, as follows.

$$\text{GDI} = \frac{A_{ro}}{A_{oo}} + \alpha \frac{A_{ri}}{A_{oi}} \tag{3}$$

where A_{ro} is the area of the outer bottom reduced by grounding damage, A_{oo} is the original area of the outer bottom, A_{ri} is the area of the inner bottom reduced by grounding damage, and A_{oi} is the original area of the inner bottom.

While equation (3) represents a ratio of the damaged area to the original area for both outer and inner bottom plate structures, α is a correction coefficient that reflects the contribution of the strength of the inner bottom structure to the ship's ultimate longitudinal strength, because the contribution of inner bottom panels to the ship's longitudinal strength differs from that of outer bottom panels. When the contribution of outer bottom panels is considered to be 100%, α representing the contribution of inner bottom panels must be smaller than 100% and it may be determined based on the variation in the ultimate longitudinal strength versus the amount of damage to the inner bottom structure.

3.4 CALCULATION OF THE RESIDUAL ULTIMATE LONGITUDINAL STRENGTH

The ultimate longitudinal strength of a ship's hull in the various damage scenarios can be calculated by a simplified or a more refined nonlinear finite element method.

The numerical computations for the individual damage scenarios selected require much computational effort. Hence, a simplified or analytical method is more useful, as long as the resulting computations are sufficiently accurate.

In this study, the modified Paik-Mansour formula method (Paik et al., 2011) is applied. This method is based on a probable bending stress distribution over the hull cross-section presumed at the ultimate limit state under vertical bending moments, as shown in Figure 9, in which h_Y is the height of the yielded area under axial tension and h_C is the height of the collapsed area under axial compression. In Paik et al. (2011), details of the benchmark studies are provided, and it was found that the mean value and the coefficient of variation in terms of the modified Paik-Mansour method calculations divided by the nonlinear finite element method computations are 0.966 and 0.063, respectively.

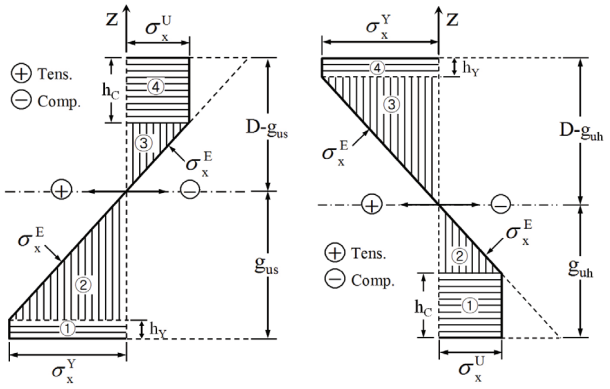

(a) Sagging (b) Hogging

Figure 9 Modified Paik-Mansour method's presumption of the bending stress distribution across the cross-section of a ship's hull at the ultimate limit state under a sagging or hogging condition (+: tension; -: compression) (the superscripts U, Y, E denote the ultimate strength, yielding, and elastic region, respectively) (Paik et al., 2011)

Ship hulls can be modeled as an assembly of plate-stiffener combination elements (i.e., stiffeners with attached plating) and/or plate-stiffener separation elements (i.e., plate elements and stiffeners).

The details of the ultimate strength formulations for plate - stiffener combinations or plate - stiffener separation models are found in Paik and Thayamballi (2003) and Hughes and Paik (2010).

Due to unsymmetry of hull cross-section associated with grounding damages, the neutral position of grounded ships with regard to horizontal and vertical axes may differ from that of intact ships. However, as long as the residual ultimate hull girder strength under vertical bending moments is concerned, hull girder collapse is considered against vertical bending moment which is applied with regard to a bending axis that is parallel to the water plane. Subsequently, the rotation of neutral axis with respect to the intact hull due to grounding damage is not taken into account.

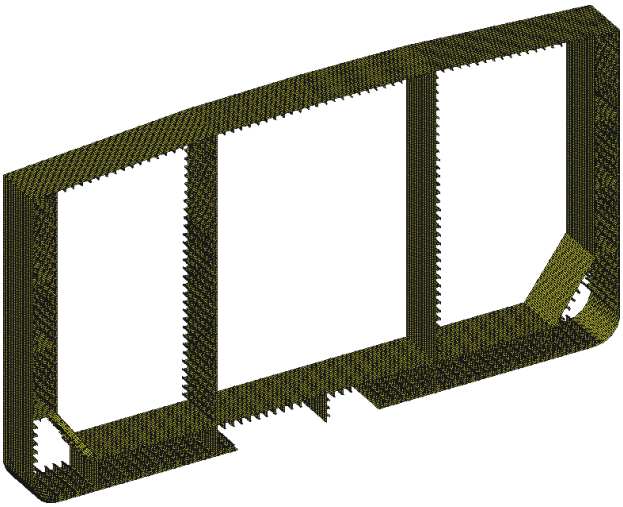

Figure 10(a) ANSYS nonlinear finite element analysis model for a VLCC class double-hull oil tanker with minor grounding damage (scenario No. 24)

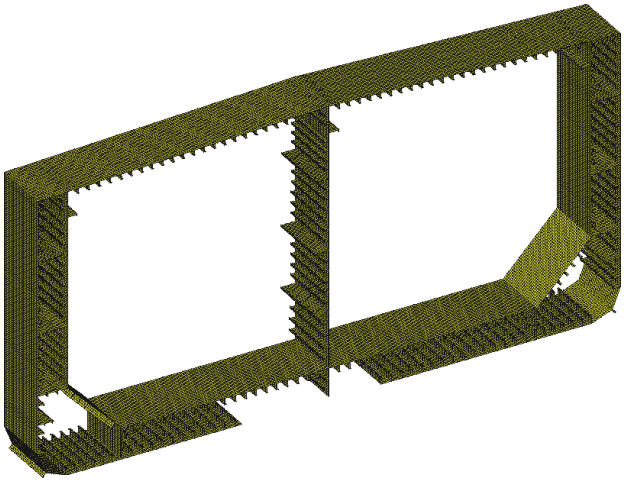

Figure 11(a) ANSYS nonlinear finite element analysis model for a Suezmax class double-hull oil tanker with minor grounding damage (scenario No. 24)

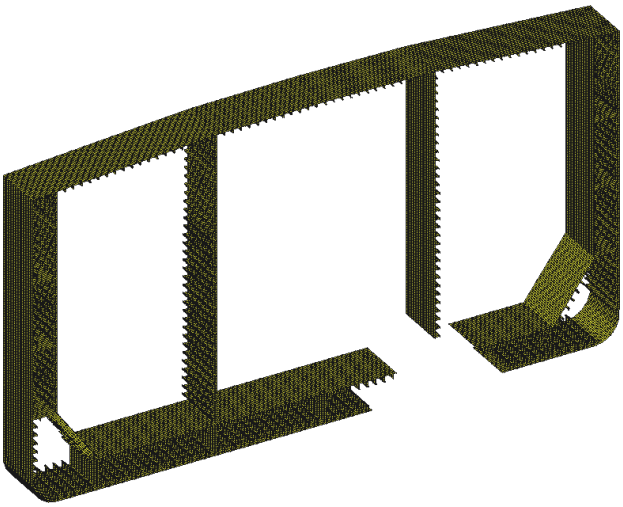

Figure 10(b) ANSYS nonlinear finite element analysis model for a VLCC class double-hull oil tanker with major grounding damage (scenario No. 35)

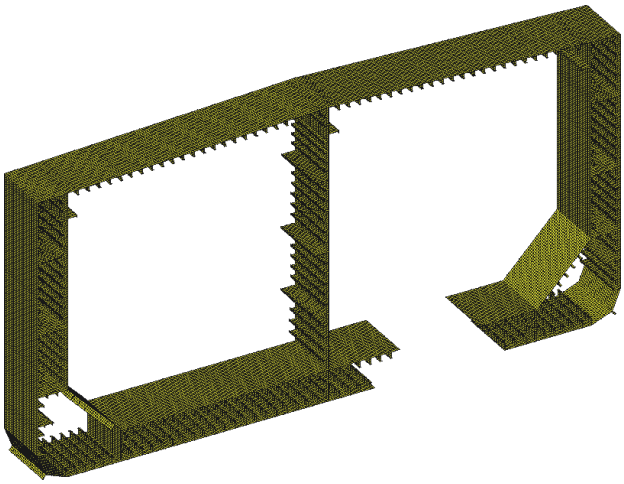

Figure 11(b) ANSYS nonlinear finite element analysis model for a Suezmax class double-hull oil tanker with major grounding damage (scenario No. 35)

The accuracy of the modified Paik-Mansour formula method for grounded ships is verified by comparing the ultimate longitudinal strength of VLCC and Suezmax class double-hull oil tankers using the ANSYS (2011) nonlinear finite element method, the ALPS/HULL (2011) intelligent super-size finite element method, and the IACS CSR (2008) Smith's method (or idealized structural unit method). Minor (small) and major (large) grounding damage scenarios and intact conditions are compared. Figures 10 and 11 present the ANSYS structural models for the vessels with minor or major grounding damage, respectively. Further details of ANSYS nonlinear finite element method modeling techniques for progressive collapse analysis of ships hulls may be referred to in Paik et al. (2011).

Figures 12 and 13 compare the ultimate longitudinal strength behavior of VLCC and Suezmax class double-hull oil tankers, respectively. The comparisons show that the Paik-Mansour formula method calculations are in reasonably good agreement for damaged ships with the results of the nonlinear finite element method using ANSYS and the intelligent super-size finite element method using ALPS/HULL. The Paik-Mansour formula method results are also compared with the IACS CSR method for intact hulls.

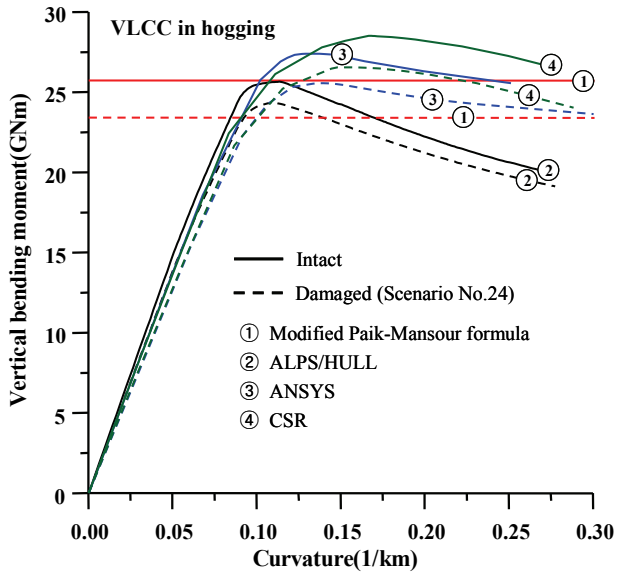

Figure 12(a) Comparison of the ultimate longitudinal strength behavior of a VLCC class double-hull oil tanker with minor grounding damage (scenario No. 24) in a hogging condition

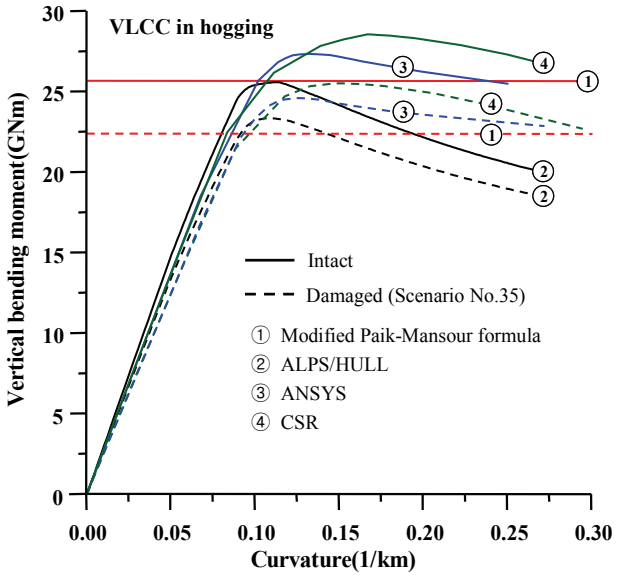

Figure 12(c) Comparison of the ultimate longitudinal strength behavior of a VLCC class double-hull oil tanker with major grounding damage in a hogging condition (scenario No. 35)

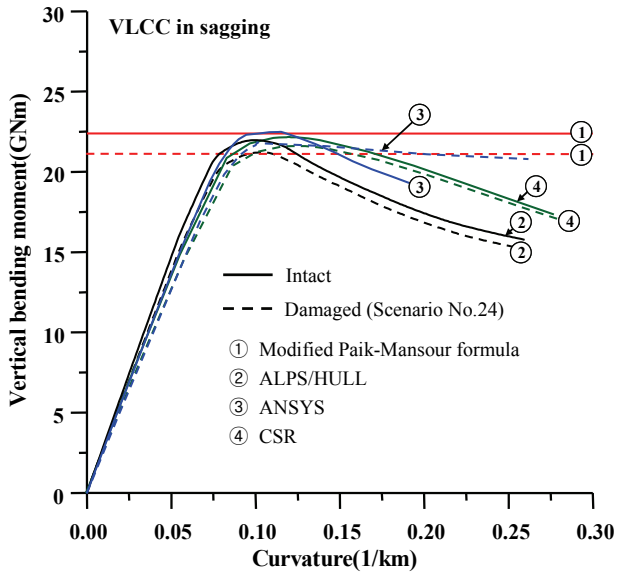

Figure 12(b) Comparison of the ultimate longitudinal strength behavior of a VLCC class double-hull oil tanker with minor grounding damage (scenario No. 24) in a sagging condition

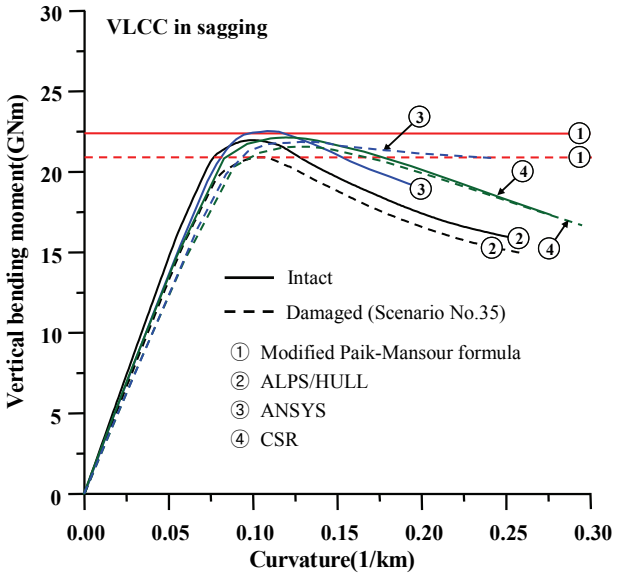

Figure 12(d) Comparison of the ultimate longitudinal strength behavior of a VLCC class double-hull oil tanker with major grounding damage (scenario No. 35) in a sagging condition

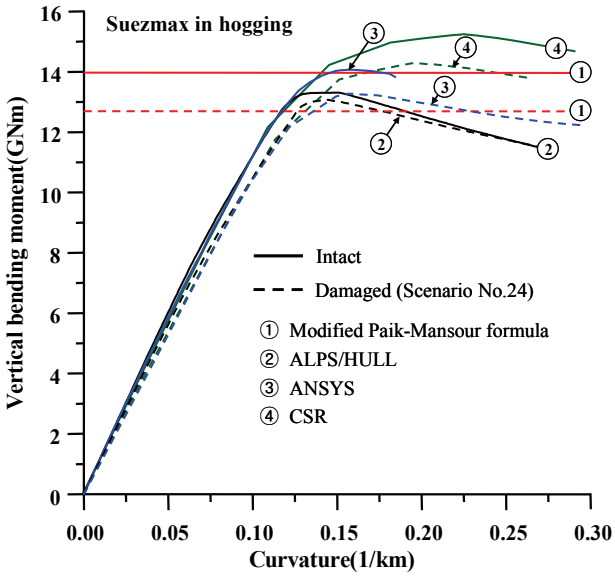

Figure 13(a) Comparison of the ultimate longitudinal strength behavior of a Suezmax class double-hull oil tanker with minor grounding damage (scenario No. 24) in a hogging condition

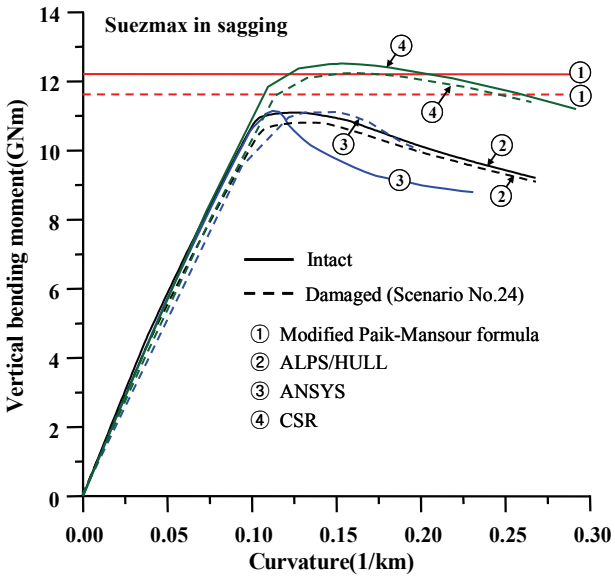

Figure 13(b) Comparison of the ultimate longitudinal strength behavior of a Suezmax class double-hull oil tanker with minor grounding damage (scenario No. 24) in a sagging condition

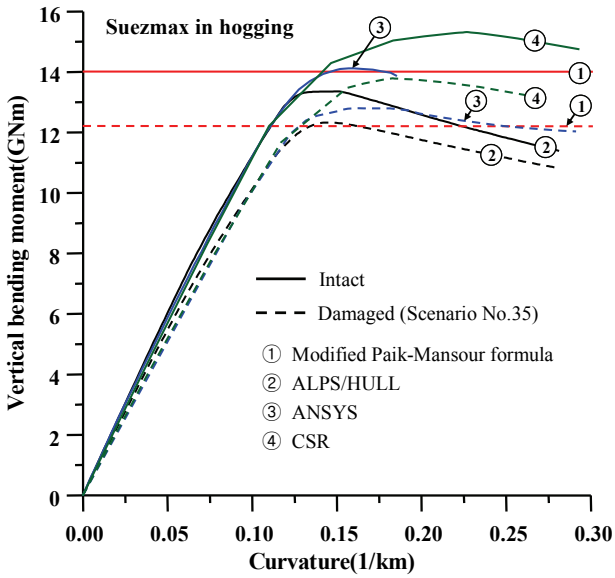

Figure 13(c) Comparison of the ultimate longitudinal strength behavior of a Suezmax class double-hull oil tanker with major grounding damage (scenario No. 35) in a hogging condition

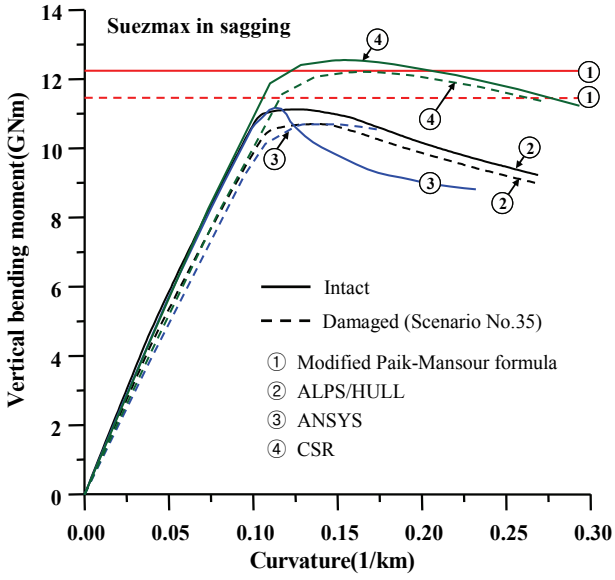

Figure 13(d) Comparison of the ultimate longitudinal strength behavior of a Suezmax class double-hull oil tanker with major grounding damage (scenario No. 35) in a sagging condition

3.5 THE R-D DIAGRAM

Once the grounding damage index and the corresponding ultimate longitudinal strength are computed for all of the selected damage scenarios, the R-D diagram can be established.

4. APPLIED EXAMPLES

4.1 OBJECTIVE SHIPS

Four types of real double-hull oil tankers − VLCC, Suezmax, Aframax, and Panamax classes − are considered to develop the R-D diagram for grounding damage. Figure 14 shows the mid-ship section designs of the four vessels, in which L = ship's length between perpendiculars, B = ship's breadth, D = ship's depth, b = double-side width, h = double bottom height. The first three ships have a similar B/D ratio of about 2.0, but the last (Panamax class tanker) has a smaller B/D ratio of 1.56.

It is assumed that the grounding damage has been suffered at mid-ship, and the R-D diagram is thus developed in association with the ultimate longitudinal strength performance of the mid-ship section. It should also be noted that the ultimate longitudinal strength of the four ships is calculated with gross scantlings, including corrosion margin values.

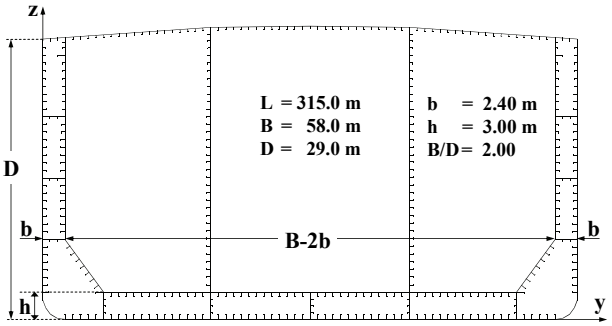

Figure 14(a) Mid-ship section design of a VLCC class double-hull oil tanker

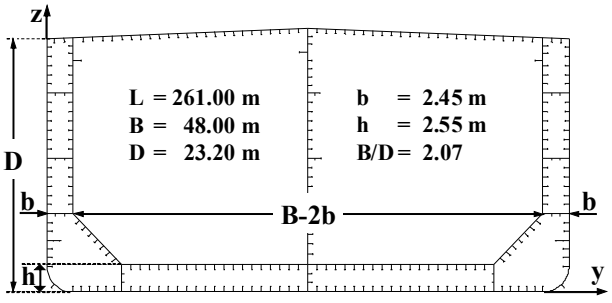

Figure 14(b) Mid-ship section design of a Suezmax class double-hull oil tanker

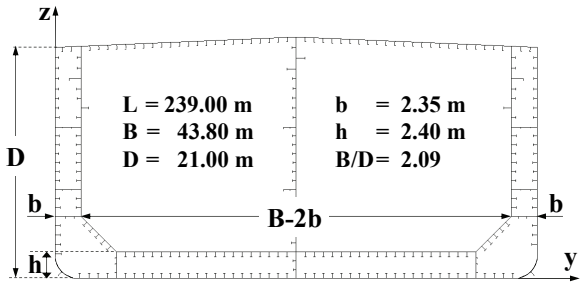

Figure 14(c) Mid-ship section design of an Aframax class double-hull oil tanker

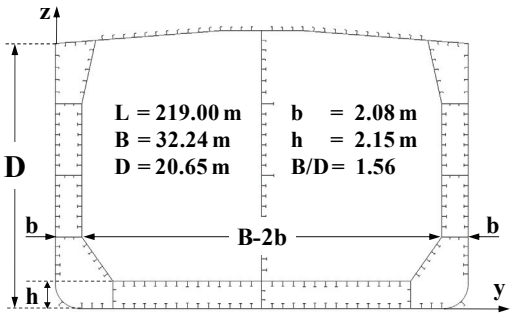

Figure 14(d) Mid-ship section design of a Panamax class double-hull oil tanker

4.2 SELECTION OF GROUNDING DAMAGE SCENARIOS

Fifty grounding damage scenarios were selected by using the Latin hypercube sampling technique. Table A.1 shows the 50 damage scenarios selected in terms of the four grounding damage parameters.

The details of the grounding damage scenarios for each vessel are determined according to the ship's geometry and dimensions and the geometry of the rock. Table A.2 represents the GDI values, which can be determined from equation (3), of 50 damage scenarios selected for each of the four double-hull oil tankers.

In some scenarios, the selected rock's angle is too large to configure the height of the grounding damage penetration. In these cases, the angle of the rock is readjusted to correspond to the height of the grounding damage penetration, with the nomenclature of Figure 3, as follows.

$$\text{If } \theta \geq 2\tan^{-1}\frac{d_1}{2H}\text{, then } \theta = 2\tan^{-1}\frac{d_1}{2H} \qquad (4)$$

Figures 15 to 18 illustrate selected grounding damage configurations for the four types of double-hull tankers. Figures A.4 to A.7 represent the probability density distributions of selected damage scenarios by a comparison with the IMO's guidance (IMO, 2003).

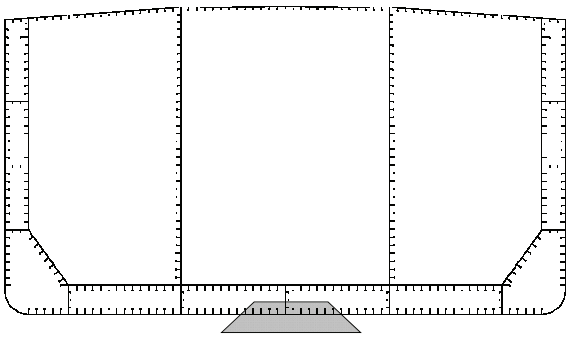

Figure 15(a) Configuration of minor grounding damage (scenario No. 26) for a VLCC class double-hull oil tanker

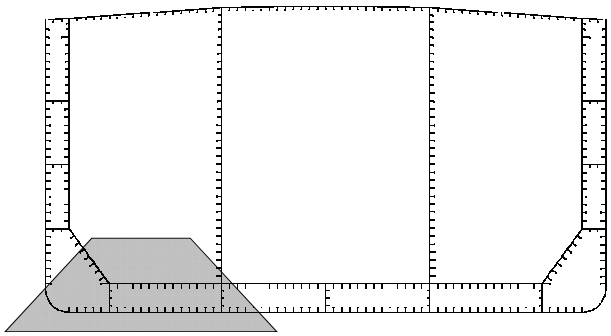

Figure 15(b) Configuration of major grounding damage (scenario No. 9) for a VLCC class double-hull oil tanker

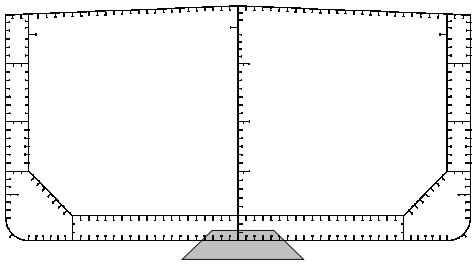

Figure 16(a) Configuration of minor grounding damage (scenario No. 26) for a Suezmax class double-hull oil tanker

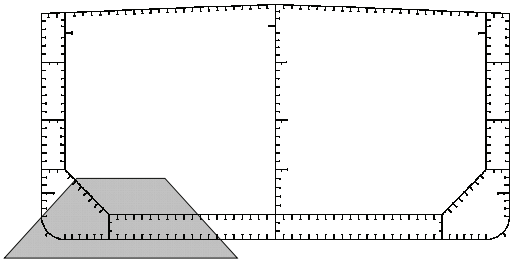

Figure 16(b) Configuration of major grounding damage (scenario No. 9) for a Suezmax class double-hull oil tanker

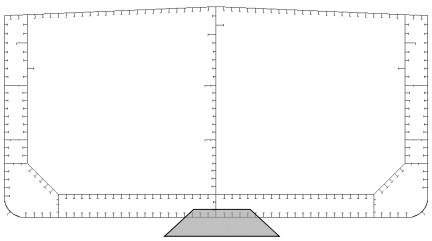

Figure 17(a) Configuration of minor grounding damage (scenario No. 26) for an Aframax class double-hull oil tanker

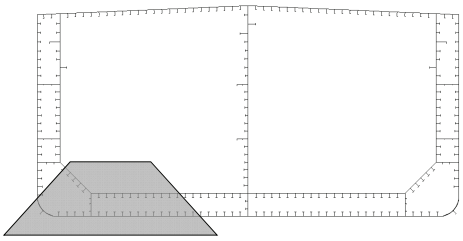

Figure 17(b) Configuration of major grounding damage (scenario No. 9) for an Aframax class double-hull oil tanker

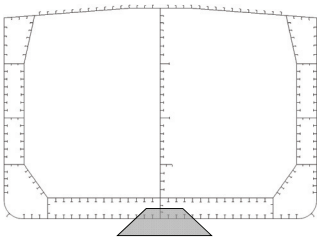

Figure 18(a) Configuration of minor grounding damage (scenario No. 26) for a Panamax class double-hull oil tanker

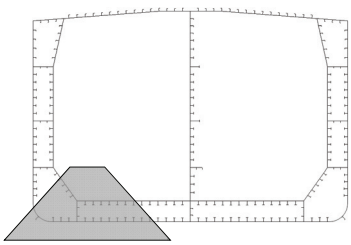

Figure 18(b) Configuration of major grounding damage (scenario No. 9) for a Panamax class double-hull oil tanker

4.3 DEFINITION OF GROUNDING DAMAGE INDEX

The grounding damage indices for individual damage scenarios can be defined from equation (3). For this purpose, the correction factor α in equation (3) must be determined in advance. Figure 19 represents the variation in M_u/M_{uo} for the four double-hull tankers in a hogging and sagging condition as the amount of damage in the

outer and inner bottom increases, where M_u and M_{uo} are the ultimate longitudinal strength of the damaged and intact ship, respectively. M_u and M_{uo} are calculated by using the modified Paik-Mansour formula method.

The correction factor α, which represents the contribution of the cross sectional area of the inner bottom to the ultimate longitudinal strength performance, can be defined as a ratio of the variation in ultimate longitudinal strength between the inner and outer bottom structures, as follows.

$$\alpha = \frac{\theta_{IB}}{\theta_{OB}}, \qquad (5)$$

where θ_{IB} and θ_{IB} are the slopes of the ultimate longitudinal strength versus the amount of grounding damage curves for the inner and outer bottom, respectively.

Table 1 summarizes the correction factors so computed for the four ships in a hogging and sagging condition.

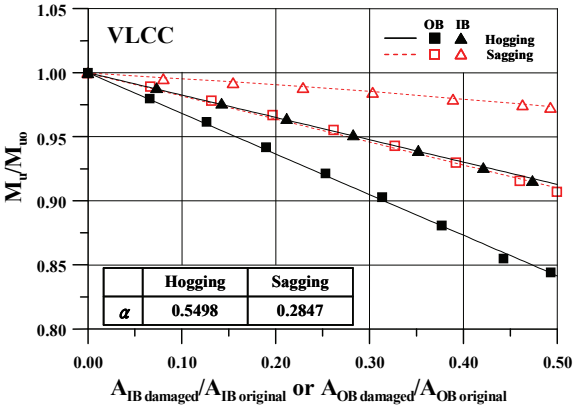

Figure 19(a) Variation in the ultimate longitudinal strength of a VLCC class double-hull oil tanker with amount of grounding damage to the outer and inner bottom

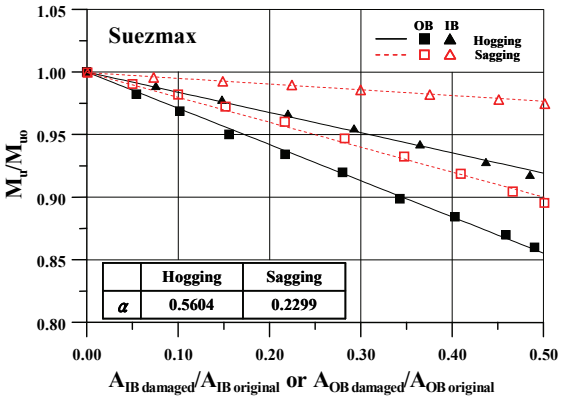

Figure 19(b) Variation in the ultimate longitudinal strength of a Suezmax class double-hull oil tanker with amount of grounding damage to the outer and inner bottom

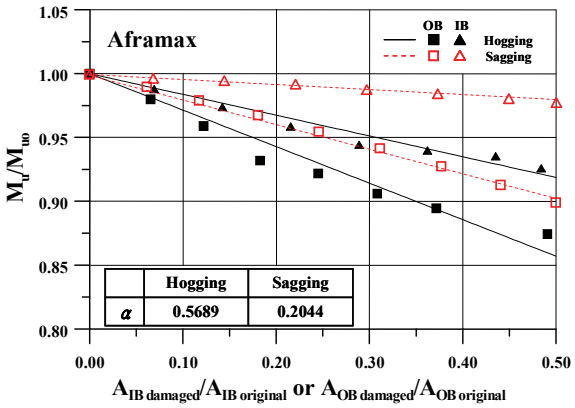

Figure 19(c) Variation in the ultimate longitudinal strength of an Aframax class double-hull oil tanker with amount of grounding damage to the outer and inner bottom

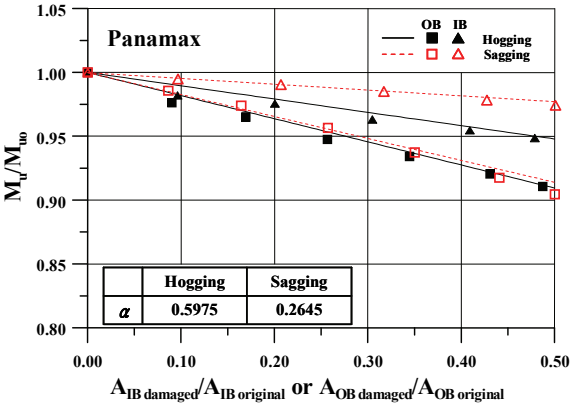

Figure 19(d) Variation in the ultimate longitudinal strength of a Panamax class double-hull oil tanker with amount of grounding damage to the outer and inner bottom

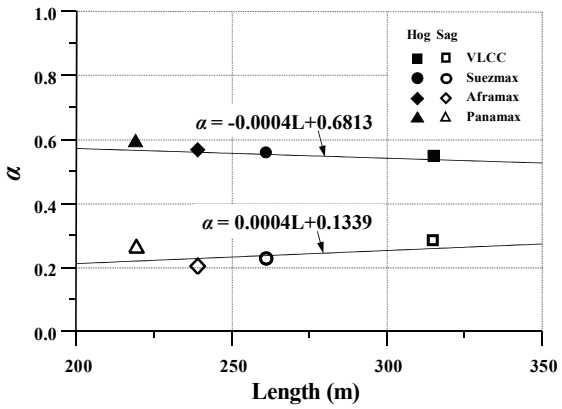

Figure 20(a) Correction factor α versus ship length

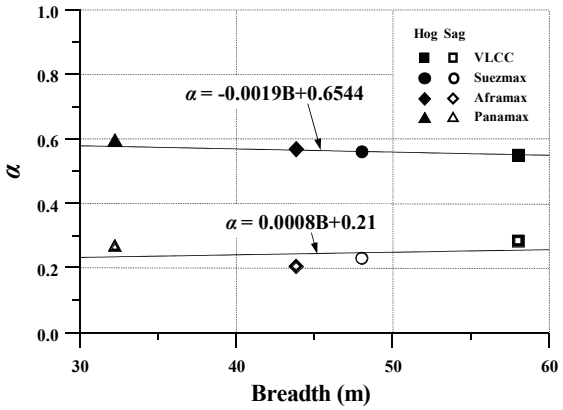

Figure 20(b) Correction factor α versus ship breadth

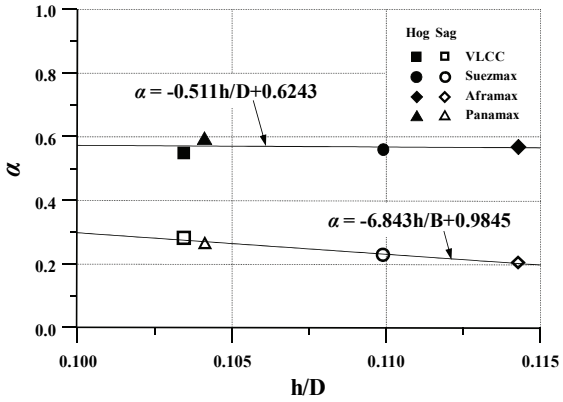

Figure 20(c) Correction factor α versus double bottom height normalized by ship depth

Table 1 Correction factor α defined for the four double-hull tankers in both a hogging and sagging condition

Tanker size	VLCC	Suezmax	Aframax	Panamax
Hogging	0.5498	0.5604	0.5689	0.5975
Sagging	0.2847	0.2299	0.2044	0.2645

It will be useful to be able to determine an identical correction factor for all vessel sizes. Figure 20 plots the correction factor versus the vessel size (e.g., ship's length, breadth, and double bottom height). Figure 20 shows that the correction factor is best formulated as a function of the ship's breadth (B) in a hogging condition and as a function of the h/D ratio in a sagging condition, by the following empirical expressions.

$$\alpha=\begin{cases}-0.0019B+0.6544 & \text{in hogging}\\ -6.843\text{h/D}+0.9845 & \text{in sagging}\end{cases}, \qquad (6)$$

With the correction factor α known, the grounding damage index can be determined from equation (3).

4.4 CALCULATION OF THE RESIDUAL ULTIMATE LONGITUDINAL STRENGTH

The residual ultimate longitudinal strengths of damaged ships in the 50 grounding damage scenarios are calculated by using the modified Paik-Mansour formula method, in which damaged structural members are removed when their contribution to the ultimate longitudinal strength performance is zero.

4.5 THE R-D DIAGRAM

Figures 21 to 24 show the residual ultimate longitudinal strength versus the grounding damage index diagrams for each of the four double-hull tankers. They show that the R-D diagrams differ with the loading direction (hogging and sagging). The diagrams can be empirically formulated as a function of the GDI, as follows.

For a VLCC class double-hull tanker:

$$\frac{M_u}{M_{uo}} = 0.0511\text{GDI}^2 - 0.3617\text{GDI} + 1.0$$

in a hogging condition (7.a)

$$\frac{M_u}{M_{uo}} = -0.2056\text{GDI}^2 - 0.1498\text{GDI} + 1.0$$

in a sagging condition (7.b)

For a Suezmax class double-hull tanker:

$$\frac{M_u}{M_{uo}} = 0.0125\text{GDI}^2 - 0.3379\text{GDI} + 1.0$$

in a hogging condition (8.a)

$$\frac{M_u}{M_{uo}} = -0.2142\text{GDI}^2 - 0.1371\text{GDI} + 1.0$$

in a sagging condition (8.b)

For an Aframax class double-hull tanker:

$$\frac{M_u}{M_{uo}} = -0.0176\text{GDI}^2 - 0.2902\text{GDI} + 1.0$$

in a hogging condition (9.a)

$$\frac{M_u}{M_{uo}} = -0.2069\text{GDI}^2 - 0.1387\text{GDI} + 1.0$$

in a sagging condition (9.b)

For a Panamax class double-hull tanker:

$$\frac{M_u}{M_{uo}} = -0.0307\text{GDI}^2 - 0.24\text{GDI} + 1.0$$

in a hogging condition (10.a)

$$\frac{M_u}{M_{uo}} = -0.1553\text{GDI}^2 - 0.1614\text{GDI} + 1.0$$

in a sagging condition (10.b)

It may be useful to present the R-D diagrams as a single representative formula for all vessel sizes. Figures 25(a) and 25(b) show R-D diagrams plotted with data from all four classes of double-hull oil tankers for hogging and sagging, respectively.

These figures show that a single formula representing all four double-hull tankers can be derived by curve-fitting as follows, as long as the amount of grounding damage is not significant.

For a hogging condition:

$$\frac{M_u}{M_{uo}} = -0.0036GDI^2 - 0.3072GDI + 1.0 \qquad (11.a)$$

For a sagging condition:

$$\frac{M_u}{M_{uo}} = -0.1941GDI^2 - 0.1476GDI + 1.0 \qquad (11.b)$$

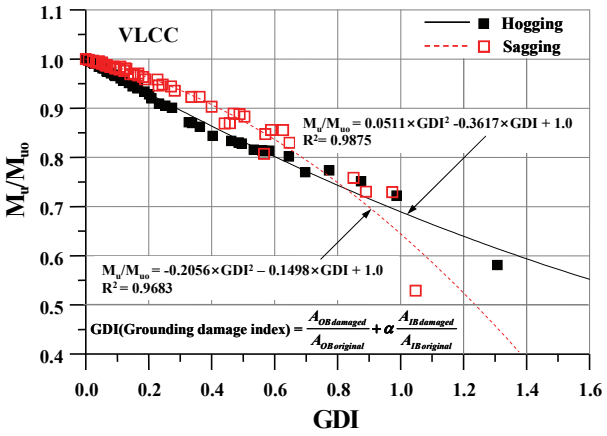

Figure 21 Residual ultimate longitudinal strength – grounding damage index diagram for a VLCC class double-hull tanker

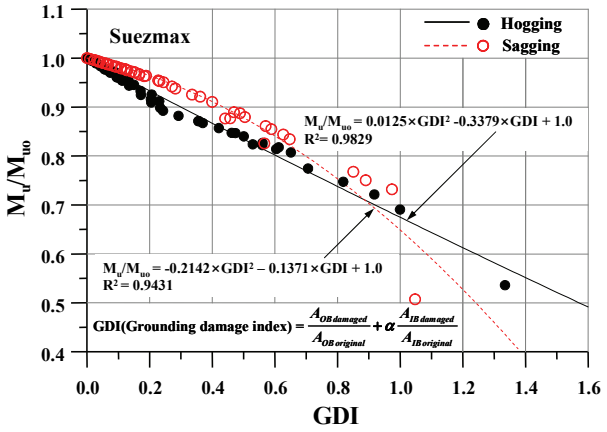

Figure 22 Residual ultimate longitudinal strength – grounding damage index diagram for a Suezmax class double-hull tanker

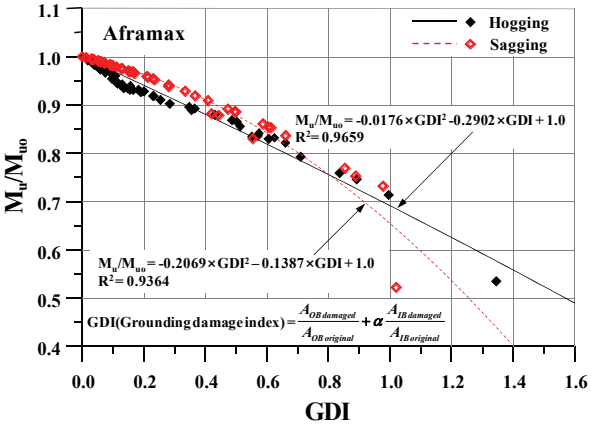

Figure 23 Residual ultimate longitudinal strength – grounding damage index diagram for an Aframax class double-hull tanker

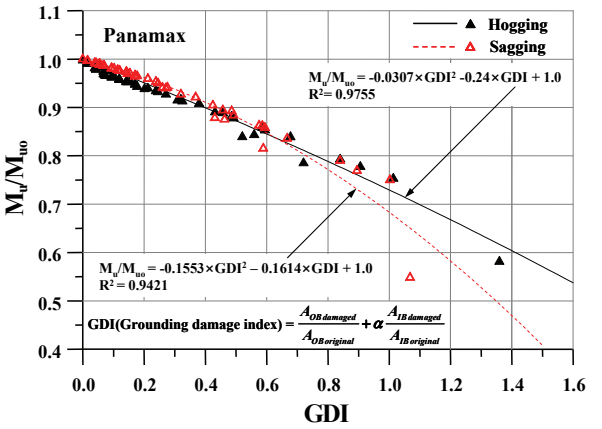

Figure 24 Residual ultimate longitudinal strength – grounding damage index diagram for a Panamax class double-hull tanker

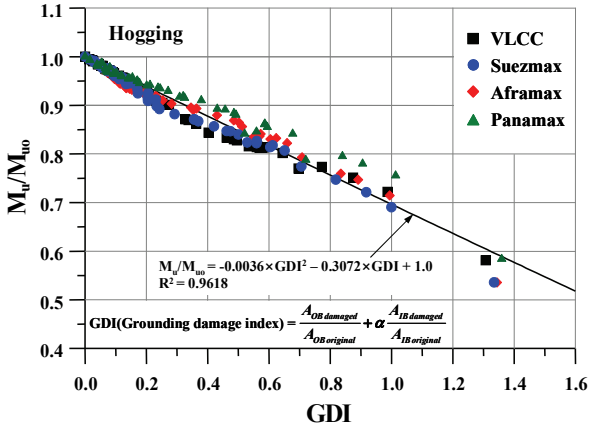

Figure 25(a) Residual ultimate longitudinal strength – grounding damage index diagram for a double-hull tanker in a hogging condition

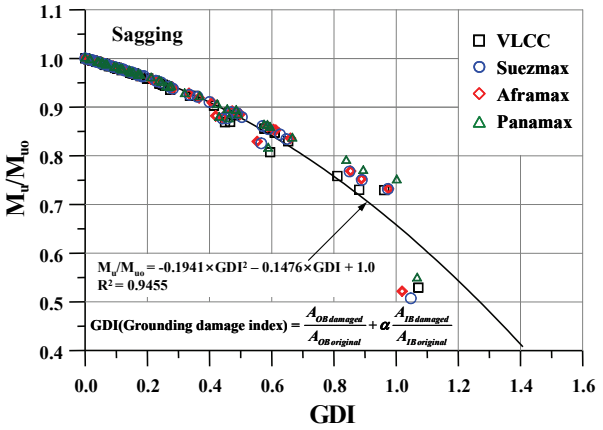

Figure 25(b) Residual ultimate longitudinal strength – grounding damage index diagram for a double-hull tanker in a sagging condition

5. POSSIBLE USES OF THE R-D DIAGRAMS

This section discusses how the developed R-D diagrams can be used in practice.

5.1 RAPID PLANNING OF SALVAGE AND RESCUE OPERATIONS

The R-D diagrams and corresponding R-D formulations developed here can be used for a first-cut estimation of the residual ultimate longitudinal strength performance of double-hull oil tankers immediately after a grounding accident has occurred where the location and amount of grounding damage is approximately known.

Figure 26 represents a schematic of the R-D diagram, showing that when the GDI value is known, the M_u/M_{uo} can be readily determined from the R-D diagram or the R-D formula.

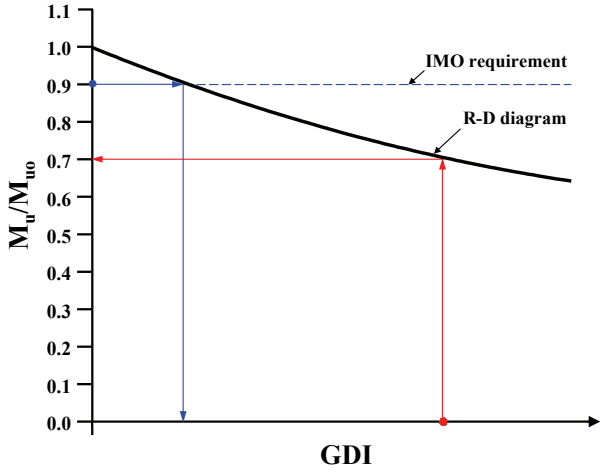

Figure 26 Use of an R-D diagram

5.2 ACCEPTANCE CRITERIA FOR GROUNDING STRENGTH PERFORMANCE

The R-D diagram can also be used to determine the acceptance criteria for grounding strength performance. As illustrated in Figure 26, the allowable grounding damage amount (grounding damage index) equivalent to the acceptance criteria for residual strength performance can be determined for any required value of residual strength.

For example, IMO (2000) specifies requirements that the ultimate longitudinal strength of all newly built ships be no smaller than 90% of the strength performance.

Table 2 Upper limits of the GDI

Tanker size	VLCC	Suezmax	Aframax	Panamax
Hog	0.2882	0.2992	0.3376	0.3965
Sag	0.4225	0.4344	0.4366	0.4363

For the double-hull oil tankers studied here, the upper limits of the grounding damage index corresponding to 90% of the ultimate longitudinal strength in a newly built condition are determined and shown in Table 2 and Figure 27. It is observed that the upper limit of the GDI tends to decrease for both hogging and sagging conditions, as ship's size increases, while the decreasing trend of the GDI's upper limit is faster in hogging than in sagging. This means that a larger ship is less endurable than a smaller ship against grounding damage.

This data presented in Table 2 is useful for developing acceptance criteria for residual ultimate longitudinal strength following grounding accidents. For example, the grounding damage amount of a VLCC class double-hull tanker should not exceed a grounding damage index value of 0.2882 in a hogging condition.

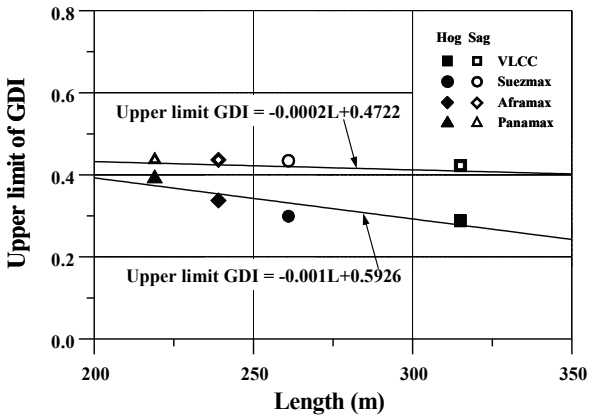

Figure 27 Upper limits of the GDI as a function of ship's length

6. CONCLUDING REMARKS

In the present paper, an innovative method has been proposed to assess the safety of ships which have suffered accidental or in-service damages. The method is formulated in terms of a residual strength versus damage index diagram (R-D diagram). To demonstrate the applicability of the proposed method, an applied example is shown in terms of R-D diagrams for double-hull oil tankers suffering grounding damage which represents diagrams between ultimate longitudinal strength versus grounding damage index. Four types of double-hull oil tankers − VLCC, Suezmax, Aframax, and Panamax − are considered.

It is concluded that the proposed method can be useful for characterizing the residual strength performance of ships as a function of the damage index. The R-D diagrams can also be employed to judge the safety level of a damaged ship in the early stages of planning for salvage and rescue operations. They will also be used to develop acceptance criteria for strength performance associated with certain amounts of accidental or in-service damage.

Further studies are being carried out to develop ultimate longitudinal strength versus collision damage index diagrams for the four types of double-hull oil tankers.

7. ACKNOWLEDGEMENTS

This study was undertaken in The Lloyd's Register Educational Trust Research Centre of Excellence at Pusan National University, Korea. This research was supported by Basic Science Research Program through the National Research Foundation of Korea (NRF) funded by the Ministry of Education, Science and Technology (Grant no.: K20902001780-10E0100-12510).

8. REFERENCES

1. ALPS/HULL (2011). A computer program for progressive collapse analysis of ship hulls, Advanced Technology Center, DRS C3 Systems, Inc., MD, USA (www.proteusengineering.com, www.maestromarine.com).
2. ANSYS (2010). Version 12.0, ANSYS Inc., Canonsburg, PA, USA.
3. IACS (2008). Common structural rules for double hull oil tankers, International Association of Classification Societies, London, UK, July.
4. Hughes, O.F. and Paik, J.K. (2010). Ship structural analysis and design, The Society of Naval Architects and Marine Engineers, New Jersey, USA.
5. IMO (2000). SOLAS/2 Recommended longitudinal strength, MSC.108(73), Maritime Safety Committee, International Maritime Organization, London, UK.
6. IMO (2003). Revised interim guidelines for the approval of alternative methods of design and construction of oil tankers, Marine Environment Protection Committee of the Organization by Resolution MEPC 110(49), International Maritime Organization, London, UK.
7. Nguyen, T.H., Garre, L., Amdahl, J. And Leira, B.J. (2011a). Monitoring of ship damage condition during stranding, Marine Structures, Vol.24, pp.261-274.
8. Nguyen, T.H., Garre, L., Amdahl, J. And Leira, B.J. (2011b). Benchmark study on the assessment of ship damage conditions during stranding, Ships and Offshore Structures, Accepted for publication.
9. Nguyen, T.H., Amdahl, J., Garre, L. and Leira, B.J. (2011c). A study on dynamic grounding of ships, Proceedings of MARSTRUCT'2011 Conference, 28-30 March 2011, Hamburg, Germany.
10. Ohtsubo, H., Kawamoto, Y. and Kuroiwa (1994). Experimental and numerical research on ship collision and grounding of oil tankers, Nuclear Engineering and Design, Vol.150, pp.385-396.
11. Paik, J.K. (2003). Innovative structural designs of tankers against ship collisions and grounding: A recent state-of-the-art review, Marine Technology, Vol.40, No.1, pp.25-33.
12. Paik, J.K. (2007a). Practical techniques for finite element modeling to simulate structural crashworthiness in ship collisions and groundings (Part I: Theory), Ships and Offshore Structures, Vol.2, No.1, pp.69-80.
13. Paik, J.K. (2007b). Practical techniques for finite element modeling to simulate structural crashworthiness in ship collisions and groundings (Part II: Verification), Ships and Offshore Structures, Vol.2, No.1, pp.69-85.
14. Paik, J.K., Amdahl, J., Barltrop, N., Donner, E.R., Gu, Y., Ito H., Ludolphy, H., Pedersen, P.T., Rohr, U. and Wang, G. (2003). Collision and grounding, Final Report of ISSC V.1, International Ship and Offshore Structures Congress, August 11-15, San Diego, USA.
15. Paik, J.K., Kim, D.K., Park, D.H., Kim, H.B., Mansour, A.E. and Caldwell, J.B. (2011). Modified Paik-Mansour formula for ultimate strength calculations of ship hulls, Proceedings of MARSTRUCT 2011 Conference, 28-30 March, Hamburg, Germany.
16. Paik, J.K. and Thayamballi, A.K. (2003). Ultimate limit state design of steel-plated structures, John Wiley & Sons, Chichester, UK.
17. Paik, J.K., Thayamballi, A.K. and Yang, S.H. (1998). Residual strength assessment of ships after collision and grounding, Marine Technology, Vol. 35, No. 1, pp. 38-54.

18. Pedersen, P.T. (2010). Review and application of ship collision and grounding analysis procedures, Marine Structures, Vol.23, pp.241-262.
19. Samuelides, M.S., Ventikos, N.P. and Gemelos, I.C. (2009). Survey on grounding incidents: Statistical analysis and risk assessment, Ships and Offshore Structures, Vol.4, No.1, pp.55-68.
20. Simonsen, B.C. and Hansen, P.F. (2000). Theoretical and statistical analysis of ship grounding accidents, Journal of Offshore Mechanics and Arctic Engineering, Vol.122, pp.200-207.
21. Wang, G., Arita, K. and Liu, D. (2000). Behavior of a double hull in a variety of stranding or collision scenarios, Marine Structures, Vol.13, pp.147-187.
22. Ye, K.Q. (1998). Orthogonal column Latin hypercubes and their application in computer experiments, Journal of the American Statistical Association, Vol.93, No. 444, pp. 1430-1439.
23. Zhang, A. and Suzuki, K. (2006). Dynamic finite element simulations of the effect of selected parameters on grounding test results of bottom structures, Ships and Offshore Structures, Vol.1, No.2, pp.117-125.
24. Zhang, S. (2002). Plate tearing and bottom damage in ship grounding, Marine Structures, Vol.15, pp.101-117.

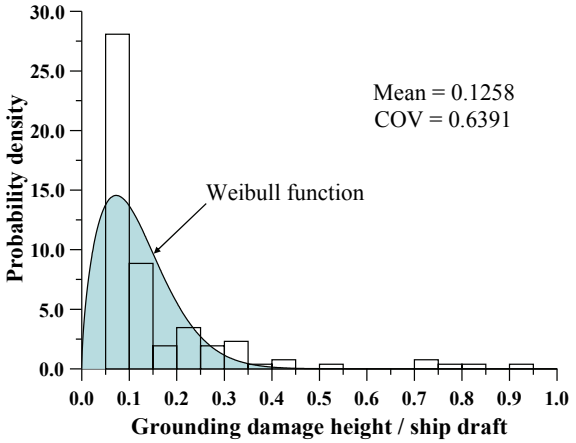

Figure A.2 Probability density distribution of grounding damage height normalized by ship draft (Paik et al., 2003)

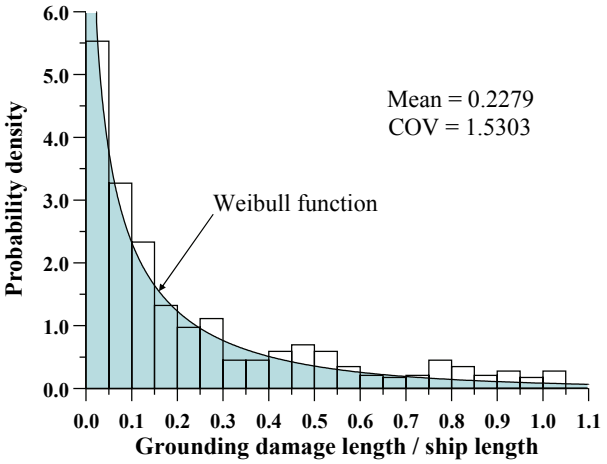

Figure A.3 Probability density distribution for grounding damage length normalized by ship length (Paik et al., 2003)

APPENDIX

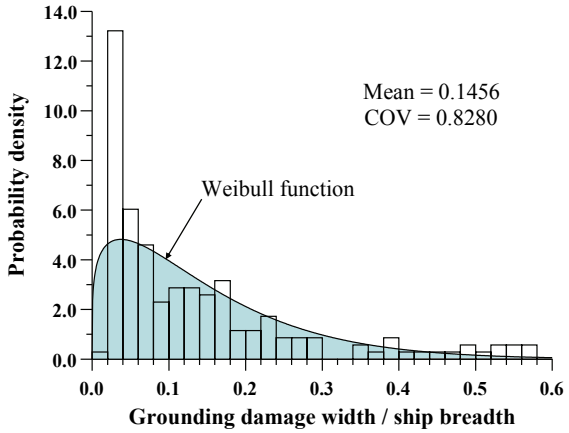

Figure A.1 Probability density distribution of grounding damage width normalized by ship breadth (Paik et al., 2003)

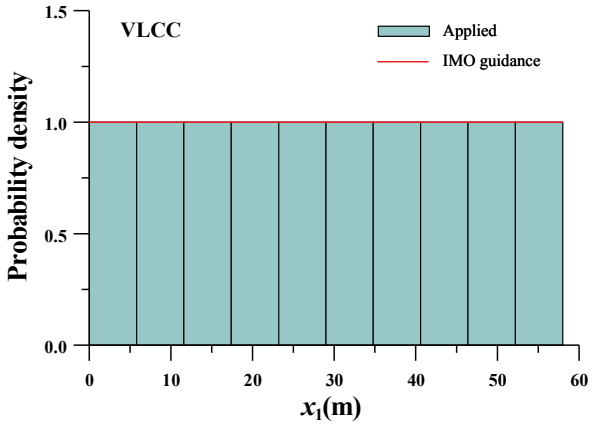

Figure A.4(a) Probability density distribution of selected scenarios for grounding damage location (x_1) of a VLCC class double-hull oil tanker (IMO, 2003)

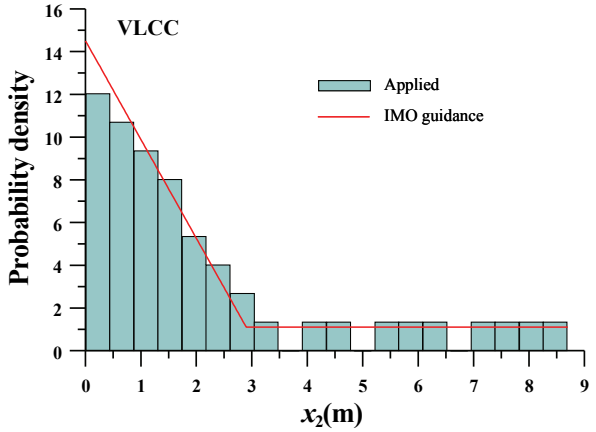

Figure A.4(b) Probability density distribution of selected scenarios for grounding damage height (x_2) of a VLCC class double-hull oil tanker (IMO, 2003)

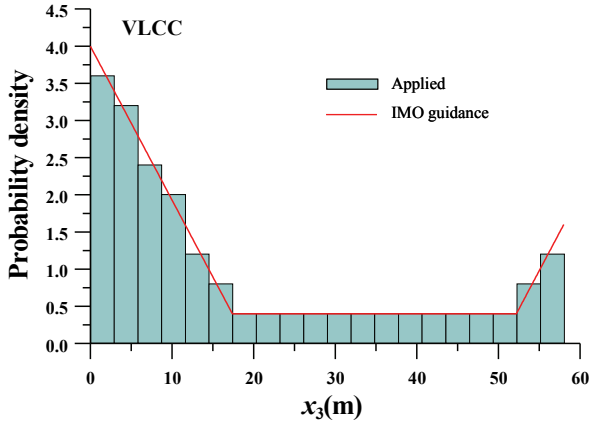

Figure A.4(c) Probability density distribution of selected scenarios for grounding damage breadth (x_3) of a VLCC class double-hull oil tanker (IMO, 2003)

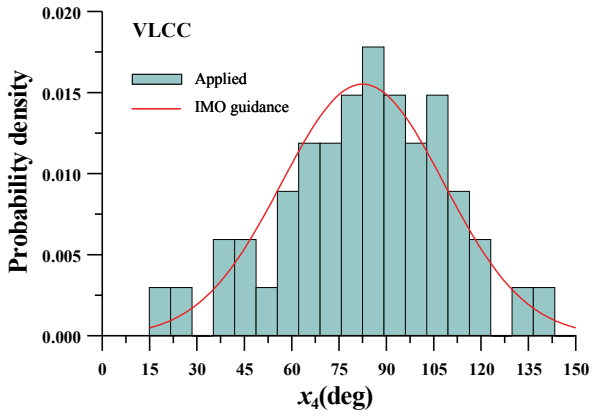

Figure A.4(d) Probability density distribution of selected scenarios for rock's angle (x_4) of a VLCC class double-hull oil tanker

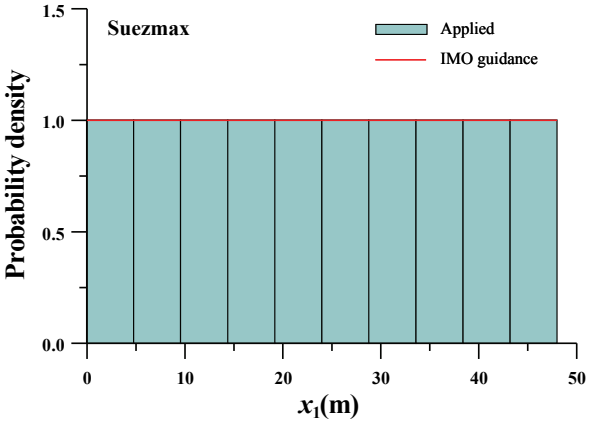

Figure A.5(a) Probability density distribution of selected scenarios for grounding damage location (x_1) of a Suezmax class double-hull oil tanker (IMO, 2003)

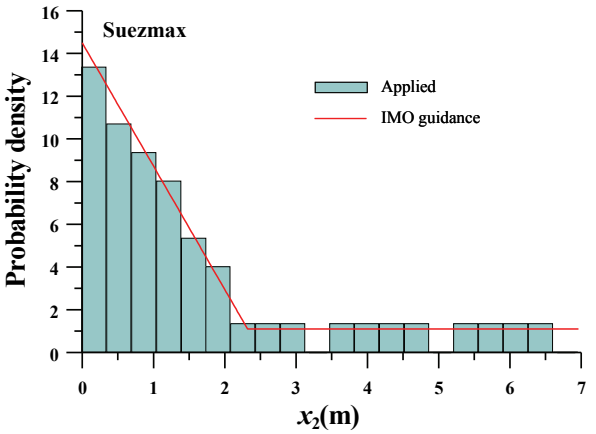

Figure A.5(b) Probability density distribution of selected scenarios for grounding damage height (x_2) of a Suezmax class double-hull oil tanker (IMO, 2003)

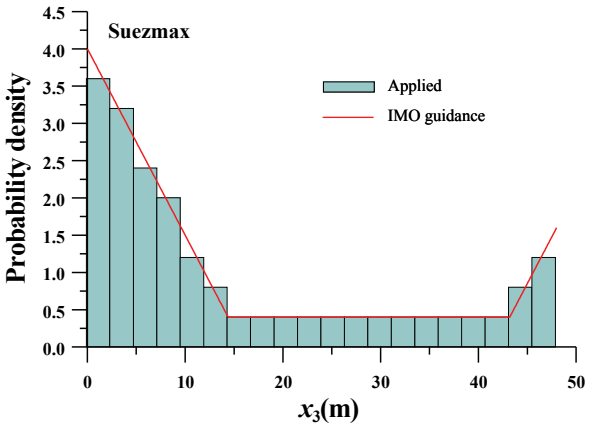

Figure A.5(c) Probability density distribution of selected scenarios for grounding damage breadth (x_3) of a Suezmax class double-hull oil tanker (IMO, 2003)

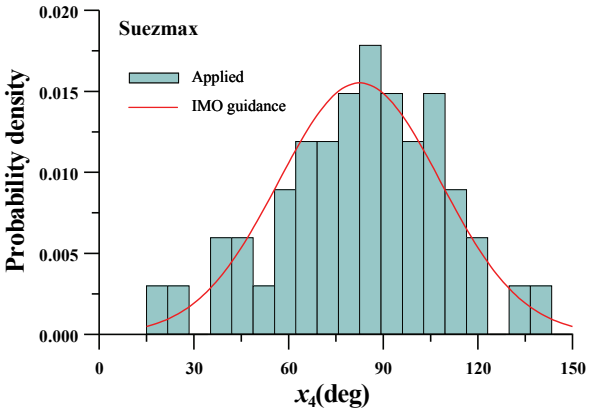

Figure A.5(d) Probability density distribution of selected scenarios for rock's angle (x_4) of a Suezmax class double-hull oil tanker

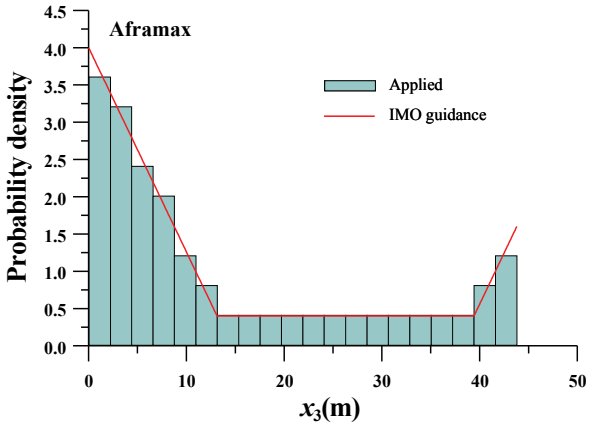

Figure A.6(c) Probability density distribution of selected scenarios for grounding damage breadth (x_3) of a Aframax class double-hull oil tanker (IMO, 2003)

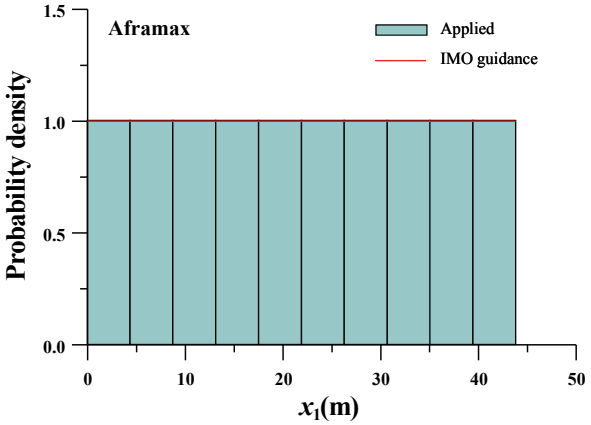

Figure A.6(a) Probability density distribution of selected scenarios for grounding damage location (x_1) of a Aframax class double-hull oil tanker (IMO, 2003)

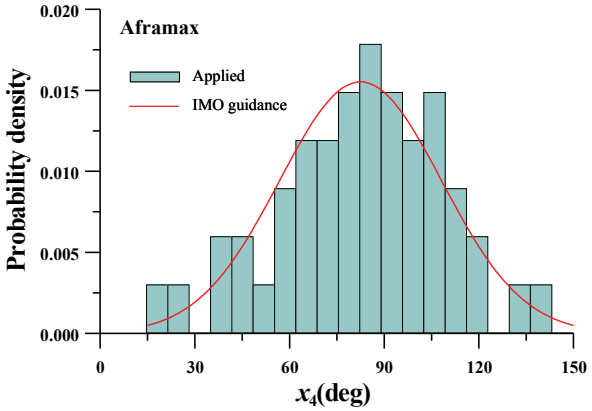

Figure A.6(d) Probability density distribution of selected scenarios for rock's angle (x_4) of a Aframax class double-hull oil tanker

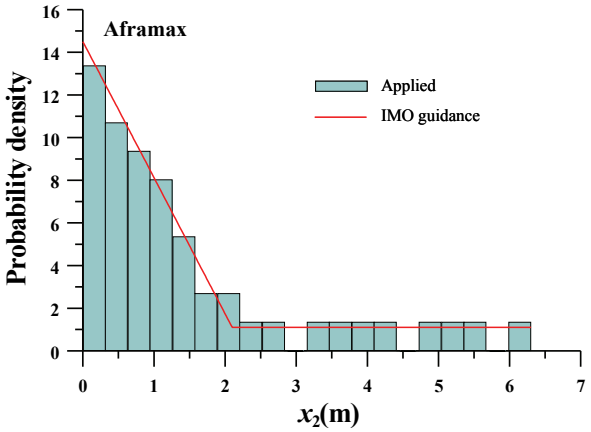

Figure A.6(b) Probability density distribution of selected scenarios for grounding damage height (x_2) of a Aframax class double-hull oil tanker (IMO, 2003)

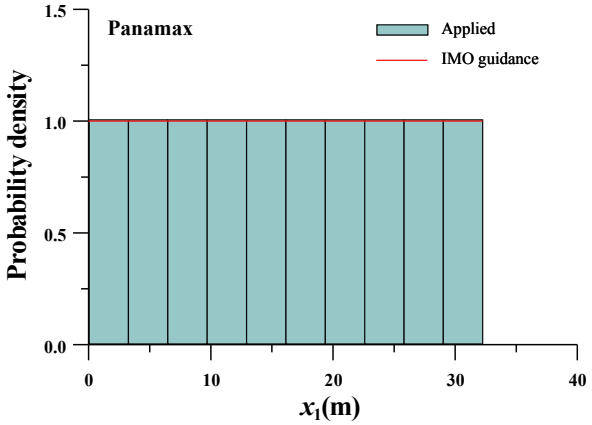

Figure A.7(a) Probability density distribution of selected scenarios for grounding damage location (x_1) of a Panamax class double-hull oil tanker (IMO, 2003)

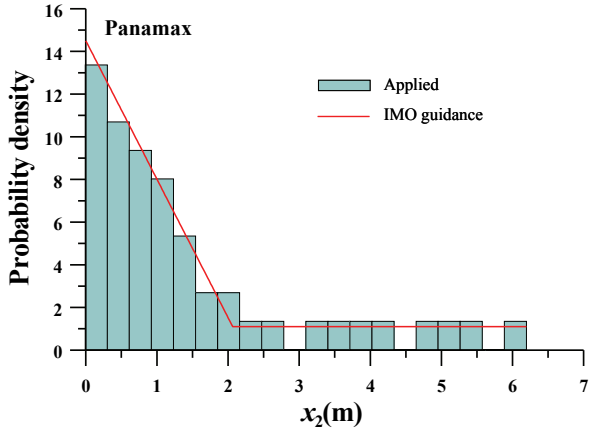

Figure A.7(b) Probability density distribution of selected scenarios for grounding damage height (x_2) of a Panamax class double-hull oil tanker (IMO, 2003)

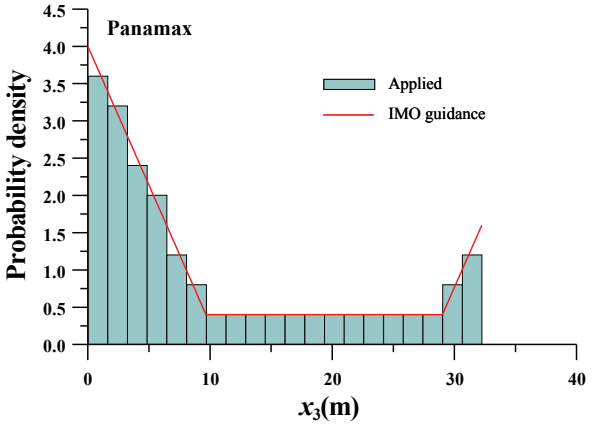

Figure A.7(c) Probability density distribution of selected scenarios for grounding damage breadth (x3) of a Panamax class double-hull oil tanker (IMO, 2003)

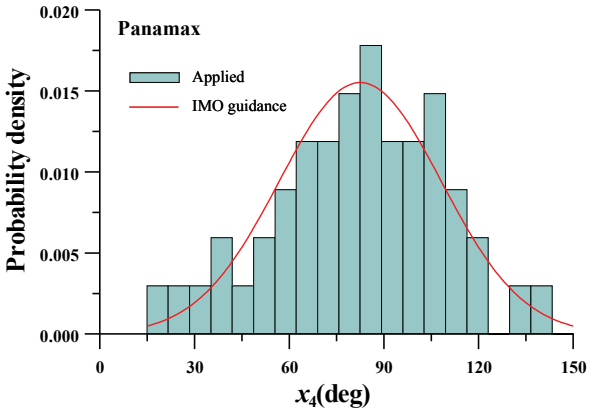

Figure A.7(d) Probability density distribution of selected scenarios for rock's angle (x4) of a Panamax class double-hull oil tanker

Table A.1 Fifty grounding damage scenarios in terms of the four grounding damage parameters

Scenario	X_1	X_2	X_3	X_4
1	0.010B	0.080D	0.144B	103.0
2	0.030B	0.017D	0.918B	88.3
3	0.050B	0.071D	0.064B	56.2
4	0.070B	0.019D	0.018B	124.0
5	0.090B	0.200D	0.777B	101.3
6	0.110B	0.016D	0.008B	74.0
7	0.130B	0.026D	0.945B	80.6
8	0.150B	0.182D	0.127B	116.5
9	0.170B	0.273D	0.427B	84.4
10	0.190B	0.219D	0.046B	96.6
11	0.210B	0.109D	0.195B	71.3
12	0.230B	0.044D	0.090B	81.9
13	0.250B	0.011D	0.023B	72.7
14	0.270B	0.008D	0.083B	99.7
15	0.290B	0.291D	0.013B	62.0
16	0.310B	0.024D	0.104B	79.3
17	0.330B	0.075D	0.327B	51.4
18	0.350B	0.033D	0.034B	53.9
19	0.370B	0.052D	0.058B	48.5
20	0.390B	0.040D	0.477B	138.7
21	0.410B	0.042D	0.577B	93.7
22	0.430B	0.255D	0.070B	87.0
23	0.450B	0.067D	0.980B	26.2
24	0.470B	0.004D	0.237B	106.7
25	0.490B	0.028D	0.003B	85.7
26	0.510B	0.049D	0.183B	92.3
27	0.530B	0.095D	0.377B	63.7
28	0.550B	0.005D	0.827B	111.1
29	0.570B	0.021D	0.153B	113.6
30	0.590B	0.038D	0.052B	75.4
31	0.610B	0.128D	0.877B	60.2
32	0.630B	0.057D	0.994B	83.1
33	0.650B	0.086D	0.097B	41.0
34	0.670B	0.006D	0.257B	89.6
35	0.690B	0.164D	0.221B	78.0
36	0.710B	0.022D	0.135B	66.9
37	0.730B	0.060D	0.727B	119.8
38	0.750B	0.036D	0.162B	76.7
39	0.770B	0.064D	0.076B	58.2
40	0.790B	0.032D	0.207B	68.4
41	0.810B	0.002D	0.119B	95.1
42	0.830B	0.014D	0.677B	98.1
43	0.850B	0.146D	0.111B	65.3
44	0.870B	0.012D	0.964B	129.8
45	0.890B	0.030D	0.040B	35.2
46	0.910B	0.047D	0.527B	104.8
47	0.930B	0.009D	0.029B	108.8
48	0.950B	0.237D	0.627B	69.9
49	0.970B	0.001D	0.172B	45.2
50	0.990B	0.054D	0.285B	91.0

Table A.2 GDI values of the four double-hull oil tankers for fifty damage scenarios selected

Scenario No.	VLCC		Suezmax		Aframax		Panamax	
	Hogging	Sagging	Hogging	Sagging	Hogging	Sagging	Hogging	Sagging
1	0.0948	0.0823	0.0900	0.0779	0.1048	0.0716	0.1104	0.0696
2	0.4622	0.4634	0.4737	0.4692	0.4851	0.4730	0.5021	0.4568
3	0.0671	0.0645	0.0746	0.0643	0.0880	0.0598	0.0908	0.0542
4	0.0419	0.0235	0.0283	0.0231	0.0181	0.0308	0.0551	0.0542
5	0.6966	0.5948	0.7057	0.5662	0.7078	0.5532	0.7069	0.5888
6	0.0241	0.0219	0.0142	0.0231	0.0181	0.0308	0.0238	0.0150
7	0.5789	0.6094	0.6120	0.5703	0.6236	0.5864	0.6193	0.5755
8	0.1867	0.1532	0.2041	0.1523	0.1998	0.1684	0.2050	0.1777
9	0.5693	0.4659	0.5595	0.4574	0.5694	0.4423	0.5536	0.4623
10	0.0795	0.0612	0.0961	0.0615	0.0985	0.0579	0.1097	0.0542
11	0.2739	0.2386	0.2334	0.2442	0.2306	0.2123	0.3411	0.2764
12	0.0928	0.1036	0.1115	0.1073	0.1130	0.0896	0.1010	0.1181
13	0.0265	0.0356	0.0573	0.0326	0.0380	0.0520	0.0512	0.0427
14	0.0904	0.0764	0.0960	0.1097	0.1147	0.0909	0.1276	0.0943
15	0.0442	0.0248	0.0506	0.0412	0.0507	0.0362	0.0437	0.0565
16	0.1107	0.1035	0.1341	0.1288	0.1346	0.1301	0.1281	0.1200
17	0.3377	0.3370	0.3553	0.3353	0.3530	0.3336	0.3492	0.3203
18	0.0530	0.0356	0.0566	0.0515	0.0577	0.0332	0.0512	0.0427
19	0.0663	0.0628	0.0743	0.0679	0.0962	0.0721	0.0764	0.0933
20	0.4853	0.4817	0.5005	0.5039	0.5123	0.4982	0.5122	0.4922
21	0.5827	0.5768	0.6041	0.6266	0.6048	0.6130	0.6309	0.5947
22	0.1185	0.0963	0.1192	0.0945	0.1281	0.0976	0.1533	0.1134
23	0.9874	0.9616	0.9995	0.9736	0.9943	0.9761	1.0219	1.0023
24	0.2327	0.2493	0.2305	0.2313	0.2533	0.2360	0.2465	0.2451
25	0.0141	0.0093	0.0291	0.0093	0.0341	0.0118	0.0223	0.0159
26	0.2085	0.2028	0.2063	0.1883	0.1895	0.2104	0.2134	0.2120
27	0.4030	0.4141	0.4207	0.3997	0.4302	0.4085	0.4048	0.4241
28	0.7728	0.8111	0.8182	0.8503	0.8344	0.8538	0.7954	0.8397
29	0.1487	0.1637	0.1500	0.1667	0.1639	0.1641	0.1726	0.1708
30	0.0683	0.0645	0.0708	0.0644	0.0741	0.0701	0.1000	0.0665
31	1.3073	1.0713	1.3346	1.0474	1.3441	1.0197	1.3622	1.0678
32	0.8744	0.8812	0.9175	0.8899	0.8914	0.8886	0.8926	0.8944
33	0.1227	0.1010	0.1128	0.1257	0.1347	0.1110	0.1276	0.1191
34	0.2523	0.2563	0.2921	0.2711	0.2824	0.2802	0.2779	0.2708
35	0.3271	0.2736	0.3568	0.2821	0.3456	0.2796	0.3619	0.2599
36	0.1372	0.1443	0.1722	0.1670	0.1532	0.1493	0.1532	0.1458
37	0.6448	0.6528	0.6510	0.6471	0.6591	0.6601	0.6702	0.6664
38	0.1637	0.1786	0.2053	0.1821	0.1891	0.1664	0.1766	0.1696
39	0.0928	0.0764	0.0944	0.0879	0.1130	0.0896	0.1010	0.0675
40	0.2011	0.1987	0.2426	0.2274	0.2306	0.2305	0.2386	0.2382
41	0.1193	0.1172	0.1388	0.1217	0.1458	0.1255	0.1200	0.1418
42	0.4957	0.4777	0.4620	0.4884	0.5018	0.4950	0.4840	0.4858
43	0.1552	0.1506	0.1709	0.1523	0.1809	0.1502	0.2050	0.1537
44	0.5601	0.5770	0.5603	0.5885	0.5731	0.6059	0.5473	0.5859
45	0.0576	0.0563	0.0429	0.0523	0.0606	0.0496	0.0677	0.0390
46	0.3626	0.3507	0.3694	0.3614	0.3637	0.3662	0.3551	0.3682
47	0.0419	0.0385	0.0488	0.0374	0.0596	0.0308	0.0551	0.0542
48	0.5339	0.4497	0.5290	0.4410	0.5502	0.4200	0.5536	0.4307
49	0.0809	0.0946	0.0772	0.0927	0.0777	0.0964	0.0789	0.1020
50	0.1653	0.1573	0.1326	0.1418	0.1553	0.1552	0.1772	0.1430